Satellite Radar Altimetry

Curt H. Davis

Abstract—**A brief review of the historical development and principles of satellite radar altimetry is presented, with special emphasis placed on the unique capability of the microwave altimeter to provide valuable information for global geoscientific studies. Altimeter data over the ocean is used to monitor mean sea levels, waveheights, windspeeds, and surface topographical features. Over the ice sheets, the altimeter data is used to produce surface elevation maps, while repeated measurements are used to monitor volume changes. The success of earlier altimeter missions has promoted the development of future missions that will provide more accurate data sets. These will continue the study of Earth's systems well into the 21st century.**

Introduction

OVER the last three decades, the development of orbiting space platforms has opened a new era in which observations of the Earth can be carried out on a global scale. Spaceborne remote sensing began in the 1960's with a series of meteorological satellites and planetary flyby spacecraft equipped with passive imaging systems. Active microwave sensors were first utilized in the 1970's aboard NASA's manned Skylab mission and the Geos-3 and Seasat satellites. In the next decade, an unprecedented number of sophisticated spaceborne remote sensing systems will be deployed to observe the Earth on a continuous basis. These measurements are designed to monitor the interactions between the ocean, atmosphere, and land, and to assess the role that each plays in a changing global environment.

Three basic types of spaceborne radar remote sensors will be used by these systems: the synthetic-aperture radar (SAR) imager, the radar scatterometer, and the radar altimeter. The microwave radar altimeter is conceptually the simplest of the active remote sensing instruments, and, after nearly two decades of spaceborne operation, it has become a well-developed and documented tool. Short-pulse altimetry from space was first suggested in the mid-1960's in a study supported by NASA at Woods Hole, MA [1]. This study drew upon the state of the art in airborne remote sensing as the basis for satellite applications. The primary purpose for the development of spaceborne altimetry was oceanic physics, where altimeters were proposed for the measurement of mean sea level and sea state. Robin [2] first proposed the use of satellite altimeters for surveying ice-sheet topography.

Manuscript received May 14, 1991; revised November 1, 1991.

The author is with the Radar Systems and Remote Laboratory, University of Kansas, 2291 Irving Hill Road, Lawrence, KS 66045.

IEEE Log Number 9107452.

The first spaceborne altimeter was flown in 1973 on NASA's manned Skylab mission [3]. It provided the experimental data that showed that meaningful oceanographic and geodetic information could be obtained from a spaceborne platform. The Geos-3 altimeter [4] operated from 1975 to 1978 and provided the spatial and temporal coverage necessary for detailed oceanographic studies. The Seasat altimeter [5], [6], which operated for three months in 1978 and then failed, is widely recognized as having made the greatest impact on the fields of oceanography and geodesy. From an orbiting altitude of 800 km, it achieved a range precision of 10 cm and has served as the model for future altimeter designs, including the U.S. Navy Geosat altimeter [7] and the European Space Agency ERS-1 altimeter [8]. In addition to oceanographic applications, the satellite altimeter has proven to be a useful tool for studying the continental ice sheets of Greenland and Antarctica [9]–[11]. In this paper, the basic principles of altimetry are discussed, and then the oceanographic and glaciological applications are reviewed.

II. Altimeter Principles and Techniques

The satellite altimeter is a nadir-pointing instrument designed to measure the precise time it takes a radiated pulse to travel to the surface and back again. If the orbital position of the satellite is known relative to a reference surface, then the measured time, converted to range, can be used to derive the elevation of the reflecting surface. A very narrow pulse (< 10 ns) is transmitted in order to obtain a small range resolution. In addition to measuring range, the altimeter records an averaged number of return echoes (typically 100), and estimates other geophysical parameters such as ocean waveheight and return pulse magnitude. A diagram of the altimeter pulse interaction with a *flat* surface and the corresponding return echo is shown in Fig. 1. As the incident pulse strikes the surface, it illuminates a circular region that increases linearly with time. Correspondingly, a linear increase in the leading edge of the return waveform occurs. After the trailing edge of the pulse has intersected the surface, the region backscattering energy to the satellite becomes an expanding annulus of constant area. At this point, the return waveform has reached its peak and then begins to trail off due to the reduction of off-nadir scattering by the altimeter's antenna pattern. For a *rough* ocean surface, the leading edge of the return pulse will be "stretched" because scattering from the wave crests precedes the scattering from

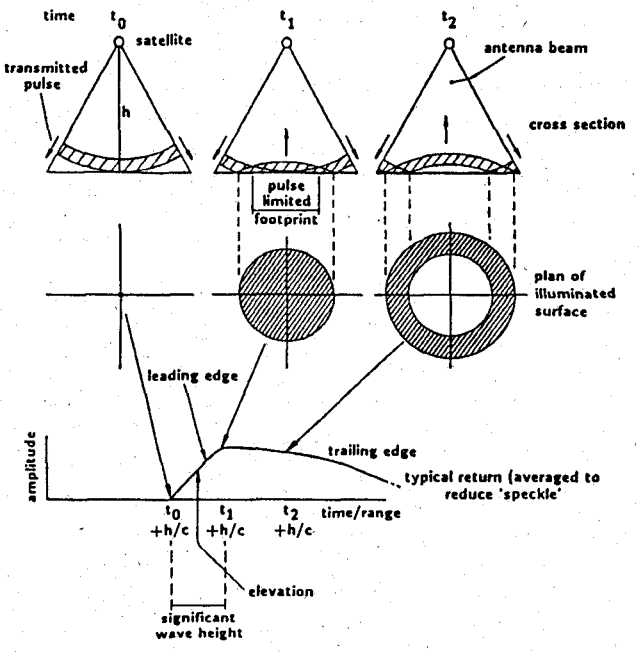

Fig. 1. The interaction of an altimeter radar pulse with a horizontal and planar surface, from its initial intersection (t_0), through the intersection of the back of the pulse shell with the surface (t_1), to the stage where the pulse begins to be attenuated by the antenna beam (t_2). The return is from the surface only (from [12]).

TABLE I
SPACEBORNE ALTIMETER CHARACTERISTICS

Parameter	Geo-3 (US)	Seasat (US)	Geosat (US)	ERS-1 (ESA)	Topex (US)
Year	1975	1978	1985	1991	1993
Range Precision (cm)	50	10	10	10	2.5
Frequency (GHz)	13.9	13.5	13.5	13.5	13.6/5.3
Pulsewidth (nsec)	12.5	3.2	3.2	3	3
Peak Power (W)	2000	2000	20	50	20/20
Orbit Altitude (km)	840	800	800	800	1334
3-dB Beamwidth (deg)	2.6	1.6	2.0	1.3	1.1/2.7
Output Amplifier	TWT	TWT	TWT	Solid-State	Solid-State
PRF (Hz)	100	1020	1020	1000	4272/1012
Max. Latitude (deg)	±65.1	±72.1	±72.1	±82	±66

TABLE II
MAGNITUDE OF DYNAMIC VARIATIONS

Source	Variation	Time Scale
Tides		
Deep Ocean	<1 m	Hours
Shallow	1–3 m	Hours
Ocean Currents		
Large Scale	1 m	Months
Mesoscale	1 m	Days
Coastal Winds	0–3 m	Hours
Surface Pressure	<0.5 m	Hours

the wave troughs as the pulse wavefront progresses downward. Thus, the width of the leading edge of the return pulse can be related to the height of the ocean waves.

A summary of important characteristics for several past and future spaceborne altimeter missions is given in Table I. The evolution of the altimeter transmitter is marked by improvements in pulse compression techniques that have substantially reduced peak power requirements. Thus, solid-state technology can be used in place of traveling-wave tube output amplifiers. All the altimeter missions listed operate at *Ku*-band. The choice of frequency is constrained by both the system and operational requirements. Since a narrow transmitted pulse (typically 3 ns) is required to achieve a reasonable range precision, high frequency operation will support both the large receiver bandwidth and narrow antenna beamwidth requirements. The upper limit on the operational frequency is constrained by atmospheric attenuation effects that significantly degrade the performance of the altimeter for frequencies >18 GHz. In addition to a *Ku*-band transmitter, the Topex altimeter will include a *C*-band transmitter so that ionospheric propagation delays can be accurately measured. The two-frequency system will produce a subdecimeter range precision so that very small dynamic variations (see Table II) in the ocean surface can be detected.

In contrast with other microwave instruments, the radar altimeter is supported by a noncontroversial mathematical model relating the return waveform to sea surface interaction. Since the backscatter area seen by the altimeter is restricted to a fraction of a degree around the nadir position, the ocean surface can be approximated by a horizontal planar surface with a large number of scattering facets distributed randomly about the mean sea surface. Moore and Williams [13] showed that the mean altimeter return waveform could be described by the convolution of two terms,

$$P_r(t) = P_\tau(t) * P_s(t) \tag{1}$$

where $P_r(t)$ is the received power at the satellite, $P_\tau(t)$ is the transmitted pulse profile, and $P_s(t)$ is a term involving the distribution of scatterers, their backscattering properties, and the antenna gain. Barrick [14] used this convolutional form and obtained a double integral describing the altimeter return waveform assuming a Gaussian distribution of scattering facets. Brown [15] approximated the transmitted pulse shape and range distribution of scatterers with Gaussian functions and generated an analytical solution for the mean ocean return. Lipa and Barrick [16] and Barrick and Lipa [17] demonstrated that the average altimeter waveform could be described by the convolution of the ocean surface specular point probability density function and a function that describes the altimeter parameters.

All on-board estimation of the oceanic geophysical parameters is based upon the ocean surface-scattering model (e.g., [18], [19]). Mean ocean-return waveforms from the Brown model are shown in Fig. 2, where each individual curve represents a different rms surface roughness, σ_s. For small σ_s, the return waveforms rise sharply to the plateau region and then begin to trail off due to the reduction in

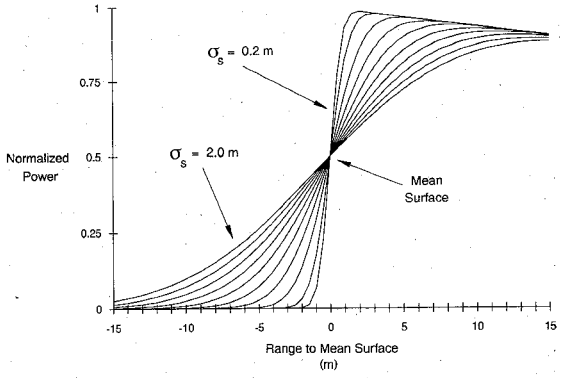

Fig. 2. Ocean surface-scatter waveforms from Brown model for different values of rms surface roughness, σ_s. Note that the half-power point corresponds to the elevation of the mean sea surface.

antenna gain at off-nadir angles. For larger and larger σ_s, the slope of the leading edge becomes shallower until the fall-off in the plateau region of the waveform is no longer apparent. Over the ocean, the width of the leading edge is used to estimate significant waveheight (SWH), where

$$SWH = 4 \cdot \sigma_s, \tag{2}$$

and the range to the mean sea surface is associated with the half-power position on the leading edge of the waveform. Since the reflectivity of the ocean surface is nearly constant, the amplitude of the return waveform can be used to estimate the surface wind speed. As the surface wind increases, the ocean surface becomes rougher and fewer areas will contribute specularly reflected energy, causing a decrease in the overall waveform amplitude. Over the last 15 years, various forms of the surface-scattering model have been used extensively to study the ocean surface, and waveheight/windspeed measurements have been validated through comparisons with *in situ* data (e.g., [20]–[24]).

The on-board algorithm that estimates the satellite range tracks the half-power point on the leading edge of the return waveform. The return waveform is digitized into equally spaced sample "gates" where the center range gate should coincide with the half-power point. The design of the tracking algorithm is based upon the assumption that the range to the surface changes slowly and predictably with time. This is a valid assumption for the ocean surface, and the algorithm positions the center gate at the half-power point very accurately. However, over the ice sheets the half-power point deviates substantially from the center gate because of larger topographical variations. Since the telemetered range corresponds to the center gate, further processing on the ground is required to correct the range estimate for ice-sheet waveforms. This procedure is called "retracking." The retracking correction is a measure of the distance of the leading edge of the return waveform from the center gate. All ice sheet altimeter data must be retracked to produce accurate elevation measurements [25], [26], and further corrections can be applied to correct for elevations errors caused by local surface slopes [27].

III. Oceanographic Applications

The oceans cover three quarters of our planet, and their dynamics play an important role in the Earth's energy and water cycles. Because water has a large heat capacity, the oceans store a major portion of the Earth's total heat content, and the transport of this energy around the globe modulates temperature and weather patterns. The oceans are the reservoir for the Earth's entire water resource, and, through circulation, evaporation, and precipitation, they regulate the global water supply. Satellite remote sensing instruments provide the only practical means for monitoring oceanographic processes on an adequate spatial and temporal scale. Satellite altimetry data over the ocean is used to globally monitor: a) the mean sea level, b) the sea state, and c) surface topographical features.

The ocean surface is a fluid interface subject to rotational and gravitational forces and is modified by atmospheric effects (wind and pressure), tides, and currents. Fig. 3 shows the relationship between the satellite height measurement, the reference ellipsoid, the marine geoid, and the sea surface elevation. In the absence of any atmospheric or tidal effects, and assuming that ocean water rotates at the same angular speed as that of the Earth, the ocean surface will follow an equipotential surface that corresponds to the mean sea level. The marine geoid is equivalent to the mean sea level and is the *static* component of the ocean surface topography. The reference ellipsoid is a smooth geometric surface that approximates the shape of the entire Earth. Because mass excesses and deficiencies produce gravity variations, the shape of the geoid is irregular, departing from the reference ellipsoid by as much as 100 m. The *dynamic* component of the ocean surface topography is primarily comprised of tides, ocean currents, and surface winds that result in elevation perturbations superimposed about the time-independent geoid (see Table II). The mean sea level is derived from averaging instantaneous elevation measurements over a long period of time. Undulations in the mean sea surface provide a wide variety of geophysical information. Long wavelength (>1000 km) variations are related to convection and subduction deep within the Earth's mantle. Medium wavelength (≈ 100–300 km) undulations are related to density inhomogeneities within the oceanic crust, and short wavelength (<100 km) undulations are directly related to the seafloor topography. Altimetric mean sea surfaces have been derived from Geos-3, Seasat, and Geosat data. Fig. 4 shows a map of the marine geoid created using three months of Seasat altimeter data. Major seafloor topographical features are clearly evident such as the mid-Atlantic ridge and the trenches in the Pacific subduction zones.

In addition to sea surface elevation measurements, satellite altimeter data can be used to describe the sea state through measurements of sea surface windspeed and ocean significant waveheight. Accurate forecasting of ocean waves and storm surges is hindered by the lack of simultaneous observations of winds and waves to test and refine

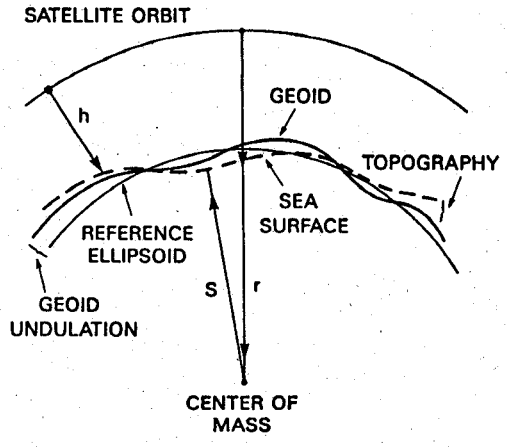

Fig. 3. Satellite altimeter observational geometry illustrating the geoid, the reference ellipsoid, the sea surface, and the dynamic ocean topography.

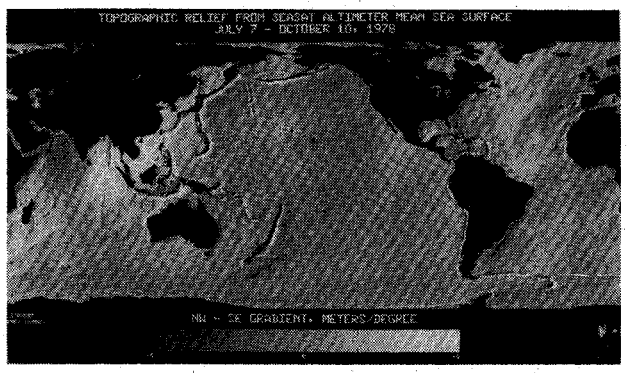

Fig. 4. Average ocean surface topography derived from Seasat altimetry data. The map shows the relationship between gravity and the shape of the sea surface. Features such as oceanic trenches, mid-ocean ridges, and seamounts are apparent. [from M. Parke, Jet Propulsion Laboratory].

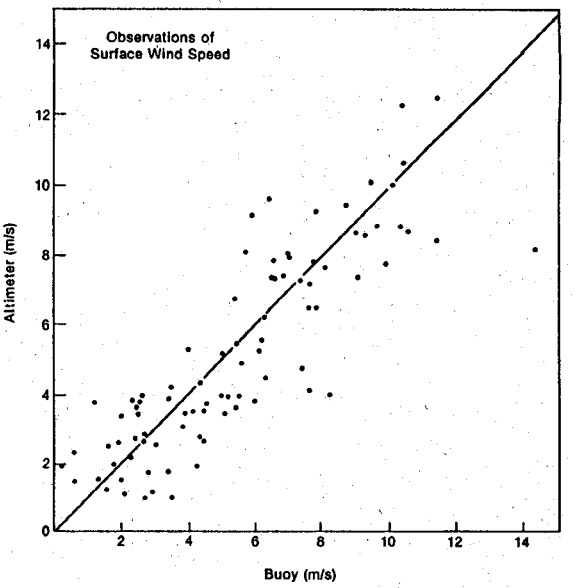

Fig. 5. Wind speed measurement derived from satellite altimeter compared to wind speed measurement made by surface buoys 10 m above the surface (from [22], Copyright © 1982, American Geophysical Union).

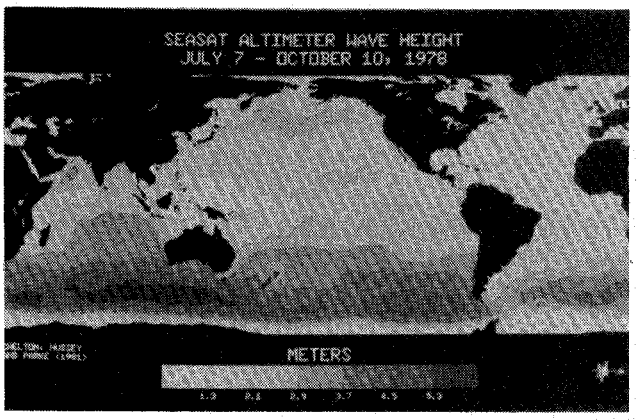

(a)

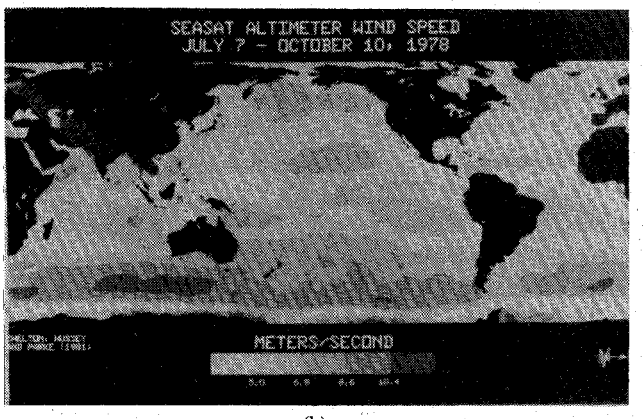

(b)

Fig. 6. (a) Seasat altimeter map of global wave heights, and (b) Seasat altimeter map of global wind speeds (from [28], reprinted by permission from *Nature*, vol. 294, pp. 529–532, Copyright © 1981, Macmillan Magazines Ltd.).

wave-prediction models. The severity of damage caused by storm surges is related to the height of the surge, which in turn is determined by complex interactions between winds, waves, and tides. Fig. 5 shows a comparison between altimeter-derived wind speeds and ocean buoy measurements made at 10 m above the surface. The overall accuracy is approximately ± 2 m/s. Fig. 6 shows global waveheight and wind speed maps derived from Seasat altimeter data. Future altimeter missions will provide continuous measurements over a period of years so that a valuable data base can be gathered to improve wave and storm forecasts.

The differences between instantaneous sea surface elevation measurements and the marine geoid are caused by dynamic variations in the ocean topography (see Fig. 3). Tides, ocean currents, and surface winds all produce substantial variations in the mean sea level. The magnitude of the elevation changes range from a few centimeters to several meters (see Table II), and extremely accurate altitude measurements are required to detect small amplitude elevation variations. Large scale currents are associated with semi-permanent oceanic circulation, while mesoscale currents are associated with time-dependent eddies. In the deep ocean basins, tides are accurately known where the variation is small, but in the shallower coastal areas the amplitude variations can reach several meters and are much less known. Fig. 7 shows a Seasat

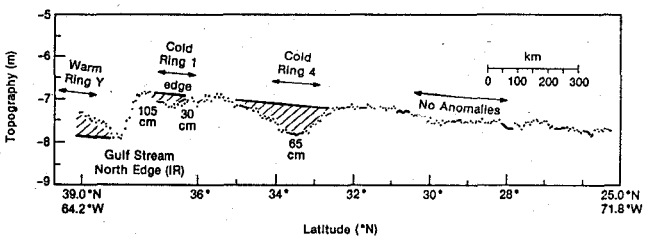

Fig. 7. Seasat altimeter elevation profile showing the gulf-stream current and two mesoscale cold rings (from [29], published in 1981 by American Geophysical Union).

elevation profile that identifies several topographical features. The gulf-stream current is clearly defined by a 1 m increase in elevation at 38°N, and two mesoscale cold rings are apparent with subsequent drops in elevation of 30 and 65 cm. Circulation patterns in the North Atlantic are fairly well known, but, by comparison, our knowledge of circulation patterns around the world is poor. By globally monitoring major topographical features such as these, our knowledge of the general circulation of the oceans can be improved so that models can be developed to help predict long-term changes brought about by a changing global climate.

IV. Glaciological Applications

Even though spaceborne altimeters were primarily designed for oceanographic applications, the orbits of Seasat and Geosat extended to latitudes of $\pm 72.1°$ (see Table I), covering major portions of the Greenland and Antarctic ice sheets. The continental ice sheets constitute 10% of the Earth's surface land area, and the accumulated ice comprises 90% of global fresh water reserves. Ice sheets exist as a consequence of climate and are coupled closely with the natural environment through complex exchanges of energy and mass. The most recent results from global climatic models predict a worldwide temperature increase of 3.0 K due to the doubling in the current levels of greenhouse gases over the next 50 years [30]. Changes in the volume of the ice sheets caused by atmospheric warming will translate directly to changes in sea level. During the last interglacial period, the sea level was 6 m higher than present-day levels. This is believed to have been caused by the total de-glaciation of the West Antarctic ice sheet [31].

The ice sheets are composed of many individual drainage basins that often show considerable independence. Localized field measurements indicate that some regions are thickening while others are thinning. This independence demonstrates that the ice sheets must be monitored in their entirety. One of the most important parameters for ice sheet studies is surface elevation. By the laws of gravity, ice flows along the direction of maximum surface slope so that elevation maps will also provide ice flow directions. Thus, elevation data can be used to define the boundaries between the major drainage basins comprising the ice sheets. Moreover, a time series of elevation measurements can be used to determine whether the ice sheets

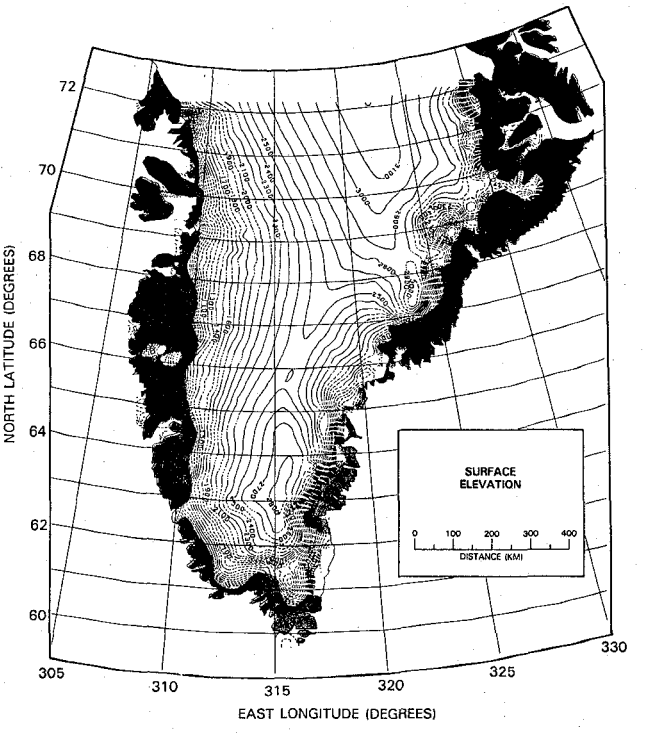

Fig. 8. Surface elevation contours of Greenland relative to mean sea level derived from Seasat altimeter data. Contour interval is 100 m (from [34]).

are growing or shrinking. Accurate determination of these rates is critical for mass balance studies that can be ultimately used to predict the response of the ice sheets to a changing global climate. Satellite altimetry provides the only proven means of measuring surface elevations with the precision and spatial coverage required for meaningful ice sheet studies [9].

Datasets produced from the Geos-3, Seasat, and Geosat satellites have been used to develop surface elevation maps of large portions of Greenland and Antarctica [32]–[34]. These measurements comprise the most comprehensive and accurate set of ice sheet elevations to date and accomplished in ten years what would have taken decades of intensive and costly field research to achieve. Fig. 8 shows surface elevation contours of Greenland south of 72.1°N with a 100-m interval derived from Seasat elevation data. The southern dome with a maximum elevation of 2800 m is evident, as well as the several drainage basins that discharge ice into the fjords of southeast Greenland. The elevation data have also been used to produce maps of specific surface features such as ice margins and ice shelves (e.g., [35]–[37]). The elevation data from all three satellites are now archived at both the World Data Center for Glaciology in Boulder, CO, and at NASA/GSFC in Greenbelt, MD. This data base allows glaciologists interested in regional studies to determine the necessary mass balance parameters, which, when combined with flow rates, provide estimates of glacial thinning or thickening.

Besides providing a reference elevation dataset, the altimeters provide a time series of data with which elevation

changes over the entire ice sheet can be determined. By comparing elevation measurements made at the same location at two separate times, one can determine any change in elevation over a specific time period. An analysis of Seasat-Geosat crossover points, spanning a decade, and also Geosat-Geosat crossover points, spanning four years, by Zwally *et al.* [38] showed that the Greenland ice sheet was thickening at an average rate of 23 cm/year. Increased precipitation rates caused by a warmer polar climate were suggested by Zwally [39] as a possible cause for the positive mass balance. This is the first direct indication of the response of the ice sheets to a changing climate and demonstrates the ability of satellite altimeters to produce results of global significance. Future altimeter missions will provide additional surface elevation data that will be used to monitor the growth rates of the continental ice sheets.

V. Conclusion

The advances in satellite remote sensing technology have had a profound effect upon the fields of oceanography and glaciology. The spaceborne radar altimeter has been utilized over the last two decades and has produced data sets that provide a combination of global coverage and temporal resolution. Future altimeter missions scheduled to fly in this decade will provide companion data sets with increased elevation precision. The major challenge that must be met is the incorporation of these observations into accurate global models describing the interaction between the ocean, atmosphere, and the ice sheets. Only in this way can we hope to accurately assess the role of the individual systems in a changing global climate.

Acknowledgment

The author wishes to thank Dr. S. P. Gogineni at the University of Kansas for his support and encouragement during the preparation of this article.

References

[1] G. C. Ewing, Ed., *Oceanography from Space.* Woods Hole, MA: Woods Hole Oceanographic Institute, ref. no. 65-10, 1965.
[2] G. de Q. Robin, "Mapping the Antarctic ice sheet by satellite altimetry," *Canadian J. Earth Sciences*, vol. 3, pp. 893–901, 1966.
[3] J. T. McGoogan, L. S. Miller, G. S. Brown, and G. S. Hayne, "The S-193 radar altimeter experiment," *Proc. IEEE*, vol. 62, pp. 793–803, 1974.
[4] H. R. Stanley, "The GEOS-3 Project," *J. Geophys. Res.*, vol. 84, pp. 3779–3783, 1979.
[5] J. L. MacArthur, "Seasat-A radar altimeter design description," *SDO-5232*, Applied Physics Lab., Laurel, MD, 1978.
[6] W. F. Townsend, "An initial assessment of the performance achieved by the Seasat-1 altimeter," *IEEE J. Ocean. Eng.*, vol. 5, pp. 80–92, 1980.
[7] J. L. MacArthur *et al.*, "The Geosat radar altimeter," *Johns Hopkins APL Tech. Dig.*, vol. 8, pp. 176–181, 1987.
[8] R. Somma *et al.*, "Radar altimeter phase A final report," ESA Contract Rep. No. CR(P)-1514, Noordwijk, Holland, 1981.
[9] R. H. Thomas *et al.*, "Satellite remote sensing for ice sheet research," *NASA Tech. Memo. 86233*, 1985.
[10] H. J. Zwally, "Technology in the advancement of glaciology," *J. Glaciology*, Special Issue, pp. 66–77, 1987.
[11] R. H. Thomas, *Polar Research from Satellites*, Joint Oceanographic Institutions, Inc., Washington, DC, 1991.
[12] J. K. Ridley and K. C. Partington, "A model of satellite radar altimeter return from the ice sheets," *Int. J. Rem. Sens.*, vol. 9, pp. 601–624, 1988.
[13] R. K. Moore and C. S. Williams, "Radar return at near-vertical incidence," *Proc. IRE*, vol. 45, pp. 228–238, 1957.
[14] D. E. Barrick, "Remote sensing of sea state by radar," in *Remote Sensing of the Troposphere*, V. Derr, Ed., Ch. 12, U.S. Government Printing Office, Washington, DC, 1972.
[15] G. S. Brown, "The average impulse response of a rough surface and its applications," *IEEE Trans. Antennas Propagat.*, vol. 25, pp. 76–74, 1977.
[16] B. J. Lipa and D. E. Barrick, "Ocean surface height-slope probability density function from SEASAT altimeter echo," *J. Geophys. Res.*, vol. 86, pp. 10,921–10,930, 1981.
[17] D. E. Barrick and B. J. Lipa, "Analysis and interpretation of altimetric sea echo," *Adv. Geophys.*, vol. 27, pp. 61–100, 1985.
[18] D. W. Hancock, R. G. Forsythe, and J. Lorell, "SEASAT altimeter sensor file algorithms," *IEEE J. of Ocean. Eng.*, vol. 5, pp. 93–99, 1980.
[19] G. S. Hayne, "Radar altimeter waveform model parameter recovery," *NASA Tech. Mem. 73294*, 1981.
[20] L. S. Fedor, T. W. Godbey, J. Gower, R. Guptill, G. S. Hayne, C. L. Rufenach, and E. J. Walsh, "Satellite altimeter measurements of sea state—an algorithm comparison," *J. Geophys. Res.*, vol. 84, pp. 3991–4001, 1979.
[21] G. S. Brown, H. R. Stanley, and N. A. Roy, "The wind-speed measurement capability of spaceborne radar altimeters," *IEEE J. Ocean. Eng.*, vol. 6, pp. 59–63, 1981.
[22] L. S. Fedor and G. S. Brown, "Waveheight and windspeed measurements from the SEASAT radar altimeter," *J. Geophys. Res.*, vol. 87, pp. 3254–3260, 1982.
[23] E. B. Dobson, "Wind and wave statistics as derived from the GEOSAT radar altimeter and comparisons with in situ measurements," *Dig. IGARSS'87*, vol. 1, pp. 245–249.
[24] F. Monaldo, "Expected differences between buoy and radar altimeter estimates of windspeed and significant waveheight and their implications on buoy-altimeter comparisons," *J. Geophys. Res.*, vol. 93, pp. 2285–2302, 1988.
[25] T. V. Martin, H. J. Zwally, A. C. Brenner, and R. A. Bindschadler, "Analysis and retracking of continental ice sheet radar altimeter waveforms," *J. Geophys. Res.*, vol. 88, pp. 1608–1616, 1983.
[26] H. J. Zwally *et al.*, "Satellite radar altimetry over ice: processing and corrections of Seasat data over Greenland," *NASA Ref. Pub. 1233*, vol. 1, NASA Scientific and Technical Information Division, 1990.
[27] A. C. Brenner, R. A. Bindschadler, R. H. Thomas, and H. J. Zwally, "Slope-induced errors in radar altimetry over continental ice sheets," *J. Geophys. Res.*, vol. 88, pp. 1617–1623, 1983.
[28] D. B. Chelton, K. J. Hussey, and M. E. Parke, "Global satellite measurements of water vapour, wind speed and wave height," Nature, vol. 294, pp. 529–532.
[29] R. E. Cheney and J. G. Marsh, "SEASAT altimeter observations of dynamic topography in the gulf stream region," *J. Geophys. Res.*, vol. 86, pp. 473–483, 1981.
[30] S. H. Schneider, "The changing climate," *Scientific American*, vol. 261, pp. 70–79, 1989.
[31] J. H. Mercer, "West Antarctic ice sheet and CO_2 greenhouse effect: a threat of disaster," *Nature*, vol. 271, pp. 321–325, 1978.
[32] R. L. Brooks, W. J. Campbell, R. O. Ramseier, H. R. Stanley, and H. J. Zwally, "Ice sheet topography by satellite altimetry," *Nature*, vol. 274, pp. 539–543, 1978.
[33] H. J. Zwally, R. A. Bindschadler, A. C. Brenner, T. V. Martin, and R. H. Thomas, "Surface elevation contours of the Greenland and Antarctic ice sheets," *J. Geophys. Res.*, vol. 88, pp. 1589–1596, 1983.
[34] R. A. Bindschadler, H. J. Zwally, J. A. Major, and A. C. Brenner, "Surface topography of the Greenland ice sheet from satellite radar altimetry," *NASA SP-503*, NASA Scientific and Technical Information Division, Washington, DC, 1989.
[35] R. H. Thomas, T. V. Martin, and H. J. Zwally, "Mapping ice sheet

margins from radar altimetry data," *Annals of Glaciology*, vol. 4, pp. 283–288, 1983.
[36] R. L. Brooks and G. A. Norcross, "Ice sheet surface features from satellite radar altimetry," *Marine Geodesy*, vol. 8, pp. 211–220, 1984.
[37] S. N. Stephenson and H. J. Zwally, "Ice-shelf topography and structure determined using satellite radar altimetry and Landsat imagery," *Annals of Glaciology*, vol. 9, pp. 162–169, 1989.
[38] H. J. Zwally, A. C. Brenner, J. A. Major, R. A. Bindschadler, and J. G. Marsh, "Growth of Greenland ice sheet: measurement," *Science*, vol. 246, pp. 1587–1589, 1989.
[39] H. J. Zwally, "Growth of Greenland ice sheet: interpretation," *Science*, vol. 246, pp. 1589–1591, 1989.

Curt H. Davis was born in Kansas City, MO, on October 16, 1964. He received the B.S. degree in electrical engineering in 1988 from the University of Kansas, Lawrence, KS.

He is currently a NASA Fellow at the Radar Systems and Remote Sensing Laboratory, University of Kansas, where he is working toward the Ph.D. degree in the area of ice sheet satellite altimetry. He has participated in two expeditions to the Antarctic continent and received the Antarctica Service Medal from the National Science Foundation. His current research interests are in the areas of microwave engineering, radar systems, and satellite remote sensing.